



Myocardial deformation analysis using cardiac magnetic resonance in apical hypertrophic cardiomyopathy: is it an useful tool to predict adverse outcomes?

Raquel Menezes Fernandes^{1,2} · Mariana Brandão³ · Ricardo Ladeiras Lopes^{3,4} · Rita Faria³ · Nuno Dias Ferreira³ · Ricardo Fontes-Carvalho^{3,4}

Received: 15 January 2023 / Accepted: 16 June 2023 / Published online: 8 July 2023
© The Author(s), under exclusive licence to Springer Nature B.V. 2023

Abstract

Apical hypertrophic cardiomyopathy (AHCM) has a broad phenotypic spectrum and still poses many diagnostic and prognostic challenges. Our team performed a retrospective study to examine the prognostic value of myocardial deformation obtained with cardiac magnetic resonance tissue tracking (CMR-TT) analysis in predicting adverse events in AHCM patients. We included patients with AHCM referred to CMR in our department from August 2009 to October 2021. CMR-TT analysis was performed to characterize the myocardial deformation pattern. Clinical, other complementary diagnostic exams characteristics and follow-up data were analysed. Primary endpoint was the composite of all-cause hospitalizations and mortality. During the 12-year period, 51 AHCM patients were evaluated by CMR, with a median age of 64 years-old and male predominance. 56,9% had an echocardiogram suggestive of AHCM. The most frequent phenotype was “the relative form” (43,1%). CMR evaluation revealed a median maximum left ventricle thickness of 15 mm and the presence of late gadolinium enhancement in 78,4%. Applying CMR-TT analysis, median global longitudinal strain was $-14,4\%$, with a median global radial strain of $30,4\%$ and global circumferential strain of $-18,0\%$. During a median follow-up of 5,3 years, the primary endpoint occurred in 21,3% of patients, with a hospitalization rate of 17,8% and all-cause mortality rate of 6,4%. After multivariable analysis, longitudinal strain rate in apical segments was an independent predictor of the primary endpoint ($p=0,023$), showing that CMR-TT analysis could be useful in predicting adverse events in AHCM patients.

Keywords Hypertrophic cardiomyopathy · Apical variant · Cardiac magnetic resonance · Tissue tracking · Myocardial strain

Introduction

Hypertrophic cardiomyopathy (HCM) is the most common hereditary myocardial disease, with a prevalence of 1:500 [1]. It is predominantly caused by mutations in sarcomeric

protein genes, with autosomal dominant inheritance and variable penetrance [2–4]. Sudden cardiac death (SCD) is the most severe complication [1].

The apical variant (AHCM) presents in 7% of HCM patients and is characterized by hypertrophy predominantly involving the apex of the left ventricle (LV) [2, 5, 6]. AHCM is more sporadic and sarcomere mutations are detected less frequently (13–30%) than in classical HCM [6]. The definition of AHCM relies on the demonstration of a LV apex wall thickness ≥ 15 mm and a ratio of maximal apical to posterior wall thickness ≥ 1.5 , based on echocardiography or cardiovascular magnetic resonance (CMR) [4, 7].

Misconceptions persist that AHCM is a benign HCM subset, but cardiovascular complications have been reported in up to one-third of these patients [2, 5, 8], including atrial fibrillation (AF), myocardial infarction, stroke, heart failure (HF), ventricular arrhythmias (VA) and SCD [2,

✉ Raquel Menezes Fernandes
ana.raquel.mf@gmail.com

¹ Cardiology Department, Centro Hospitalar Universitário do Algarve – Hospital de Faro, Faro, Portugal

² Algarve Biomedical Center, Faro, Portugal

³ Cardiology Department, Centro Hospitalar de Vila Nova de Gaia/Espinho, Vila Nova de Gaia, Portugal

⁴ Cardiovascular R&D Centre - UnIC@RISE, Department of Surgery and Physiology, Faculdade de Medicina da Universidade do Porto, Porto, Portugal

7–9]. Development of apical aneurysm or mid-ventricular obstruction have also been shown to increase the risk of SCD and progression to end-stage HF in AHCM [10, 11].

Echocardiography is typically the initial imaging modality used in the evaluation of AHCM [3, 7, 12], with the “ace-of-spades” configuration of the LV cavity in diastole as the diagnostic hallmark [7]. However, in the absence of contrast enhancement, the diagnostic accuracy is limited, resulting in an underestimation of the maximal wall thickness [2, 3, 5]. Moreover, LV apical aneurysms are frequently missed by echocardiography [3]. CMR provides the most reliable characterization of the location, distribution, extent of LVH and presence of apical aneurysms in AHCM [3, 7, 13, 14]. The presence and extent of late gadolinium enhancement (LGE) may be associated with an increased risk of HF, VA and SCD [1, 4, 15]. Decreased myocardial strain evaluated by deformation imaging is associated with extensive myocardial fibrosis and poor prognosis in HCM [14, 15]. CMR tissue tracking (CMR-TT) can quantitatively measure myocardial strain from radial, circumferential, and longitudinal directions based on the cine views, reflecting the global and regional left ventricular function [1]. It is a promising technique to detect subclinical myocardial deformation in various cardiovascular diseases, with high sensitivity and reproducibility [16].

In this study, we aimed to analyse myocardial deformation patterns obtained with CMR-TT analysis, and its value in predicting adverse outcomes in AHCM patients.

Methods

Study population and endpoint

We conducted a single-centre retrospective study, including 51 consecutive patients referred to the Cardiovascular Imaging Department of Centro Hospitalar de Vila Nova de Gaia/Espinho for CMR evaluation due to clinically suspected AHCM, from August 2009 to October 2021. CMR-TT analysis was performed to each patient to characterize the myocardial deformation pattern.

We further analysed baseline characteristics and other complementary diagnostic exams characteristics, as well as follow-up data. AHCM was also subclassified into three forms: (1) “pure,” with isolated apical LV hypertrophy (LVH); (2) “mixed,” with predominantly apical, but also interventricular septal hypertrophy; and (3) “relative” AHCM, with loss of the progressive tapering of myocardial wall thickness towards the apex, although failing to reach the AHCM diagnostic cut-off of wall thickness ≥ 15 mm^{4,7}. The presence of VA was defined as previous aborted cardiac arrest, documented sustained ventricular tachycardia and

non-sustained VT (NSVT). The primary endpoint was the composite of all-cause hospitalizations and mortality.

The study was conducted in accordance with the Declaration of Helsinki and was approved by the local Ethics Committee. The requirement for written informed consent was waived due to the retrospective nature of the study.

Cardiac magnetic resonance: imaging acquisition and analysis

Datasets from a total of 46 patients with AHCM were finally included in TT analysis; five patients were excluded due to severe motion artifacts on cine imaging. All CMR views were performed on 1.5-T magnetic resonance Siemens scanner (MAGNETOM Symphony TIM, Siemens Medical Solutions, Erlangen, Germany). Cine images for functional and TT analyses were acquired in two/three/four-chamber views, and in short-axis (SAX) views using a steady-state free precession sequence during breath-hold and with retrospective ECG triggering (repetition time/echo time: 2.4/1.2 ms; flip angle: 60 degrees; in-plane resolution 1.4 mm×1.4 mm; slice thickness: 8 mm). Typically, the number of reconstructed phases was 30 and the number of segments was adjusted aiming for a temporal resolution of 20–40 ms. LGE images were acquired approximately 10–15 min after a 0,2 mmol/Kg gadolinium bolus administration, using a segmented gradient echo inversion recovery sequence. Two or three physicians experienced in CMR analysed the data and performed the measurements. Images were post-processed using commercially available software (cvi42, Circle Cardiovascular Imaging Inc., Calgary, Canada).

Epicardial and endocardial borders of the LV myocardium were manually traced in end-diastolic and end-systolic phases on SAX cine images to calculate functional parameters: LV ejection fraction, LV end-diastolic volume, indexed LVEDV, LV end-systolic, indexed LVESV, LV mass and indexed LV mass. Papillary muscles were included in the left ventricular cavity volume. The long-axis images and SAX stack were viewed simultaneously to cross-check for the presence of WMA and LGE.

A set of long-axis (two/three/four-chamber) and SAX views were loaded into the tissue tracking module to analyse myocardial strain (Fig. 1), which referred to the degree of myocardial deformation from its initial length (L_0 , usually in the end diastole) to its maximum length (L , usually in the end systole) and was expressed as a percentage: $(L - L_0)/L \times 100\%$. It includes GLS, global radial strain (GRS) and global circumferential strain (GCS). The endocardial border and the epicardial border were automatically detected and manually adjusted if deemed inadequate. An average of the measurements of three SAX views enabled calculation

of global peak systolic radial strain, strain rate, velocity and displacement, and global peak systolic circumferential strain and strain rate (Fig. 1). Global peak systolic longitudinal strain, strain rate, velocity and displacement were derived from the measurements of the 4-, 2- and 3-chamber cine images.

Statistical analysis

Descriptive data was summarized using the appropriate statistical tools, given the nature of the variables involved. Categorical variables were described as absolute frequencies (n) and relative frequencies (%). Median and percentiles or mean and standard deviation were used for continuous variables, according with data distribution. Student *t* test or its non-parametric equivalent (Mann-Whitney *U* test) were used to compare the distribution of continuous variables. Pearson’s χ^2 test was used to test an hypothesis about categorical variables.

Multivariable logistic regression modeling was performed to identify predictors of the primary endpoint. The effect of the variables was assessed by estimating the hazard ratio (HR) and respective confidence intervals. The significance level used was 0,05. Statistical analysis was

performed using the software Statistical Package for the Social Sciences v. 23.0 (IBM SPSS, Armonk, New York, USA).

Results

Baseline characteristics

During the 12-year period, 51 patients with AHCM, with a median age of 64 years-old and male predominance (60,8%), were evaluated by CMR. Table 1 describes the baseline characteristics of the population. Family history of HCM or SCD was present in 7,8%. T-wave inversion on precordial ECG leads was found in 78,4% of patients. Transthoracic echocardiogram (TTE) was previously performed in 47 individuals (92,2%), but only in seven patients was administered ultrasonographic contrast. In 56,9%, TTE was suggestive of AHCM. The most frequent AHCM phenotype was the “relative form” (43,1%), followed by the “pure apical form” (37,3%) and the “mixed form” (17,6%).

Cardiac magnetic resonance characterization

Table 2 outlines the CMR characterization. Median maximum LV thickness was 15 mm, with a median LV mass

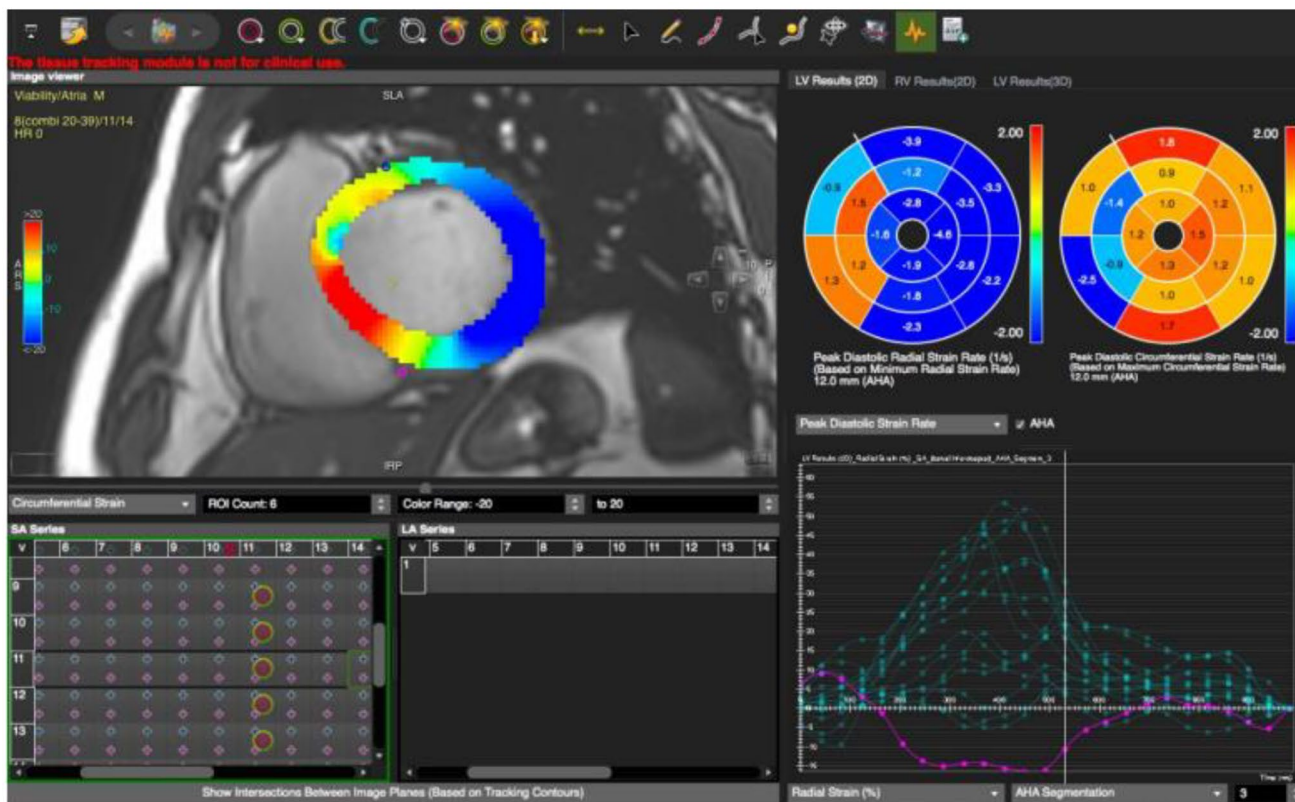


Fig. 1 Tissue tracking tool application to analyse myocardial strain in short-axis view. (adapted from cvi42® - User manual Version 5.5 [17])

Table 1 Baseline characteristics of the AHCM patients

Clinical Characteristics	Total n = 51
Age (years-old), median	64
Male gender, n (%)	31 (60,8%)
Arterial hypertension, n (%)	32 (62,7%)
Diabetes mellitus, n (%)	15 (29,4%)
Atrial fibrillation, n (%)	8 (15,7%)
Coronary artery disease, n (%)	6 (11,8%)
Valvular heart disease, n (%)	0 (0%)
Chronic kidney disease, n (%)	2 (3,9%)
Familiar history of HCM, n (%)	4 (7,8%)
Familiar history of SCD, n (%)	4 (7,8%)
Chest pain, n (%)	14 (27,5%)
Fatigue, n (%)	17 (33,3%)
Palpitations, n (%)	7 (13,7%)
Syncope, n (%)	2 (3,9%)
Body mass index (kg/m ²), median	26,9
Left ventricular hypertrophy in ECG, n (%)	4 (7,8%)
T-wave inversion in ECG, n (%)	40 (78,4%)

ECG = Electrocardiogram; HCM = Hypertrophic cardiomyopathy; SCD = Sudden cardiac death

Table 2 CMR characterization of AHCM patients

CMR parameters	Total n = 51
Maximal LV thickness (mm), median	15
LV mass index (g/m ²), median	76
End-diastolic LV volume index (ml/m ²), median	78,5
End-systolic LV volume index (ml/m ²), median	25
Left ventricle ejection fraction (%), median	66
Cardiac index (L/min/m ²), median	3,25
Systolic volume index (ml/m ²), median	51,5
Left atrium volume index (ml/m ²), median	55
Apical aneurysm, n (%)	1 (2%)
Late gadolinium enhancement, n (%)	40 (78,4%)
• Apical localization, n (%)	37 (92,5%)
• Other regions, n (%)	3 (7,5%)
• Affected segments, median	5

AHCM = Apical hypertrophic cardiomyopathy; CMR = Cardiac magnetic resonance; LV = Left ventricle

index of 76 g/m² (Fig. 2). LGE was present in 78,4%, with a median of five affected LV segments (Fig. 3). CMR-TT analysis revealed a median global longitudinal strain of -14,4%, with a median global radial strain of 30,4% and a global circumferential strain of -18,0% (Table 3).

Adverse events

On 24-Holter monitoring, 21,6% of patients presented NSVT; no sustained VA were registered. During a median follow-up of 5,3 years, the primary endpoint occurred in 10 patients (21,3%), with a hospitalization rate of 17,8% (cardiac causes in 2%) and all-cause mortality rate of 6,4%. Those patients were older (69,2 vs. 59,5 years-old; $p=0,01$),

had a larger prevalence of chronic obstructive pulmonary disease (COPD) (20% vs. 2,7%; $p=0,047$), and lower longitudinal strain rate in apical segments (0,27 vs. -0,74 s⁻¹; $p=0,021$) (Table 4). After multivariable analysis, only longitudinal strain rate in apical segments was an independent predictor of the primary endpoint (HR = 5,62 [1,25–25,3], $p=0,023$). Even after excluding the patient with the apical aneurysm, this parameter remained an independent predictor of the primary endpoint (HR = 4,58 [1,13–18,571], $p=0,033$). Neither parameter regarding LGE reached statistical significance, namely apical involvement or by number of segments affected. Four patients (7,8%) were lost to follow-up and were not included in the endpoint analysis.

Discussion

To our knowledge, this study is the first addressing myocardial deformation parameters derived by CMR-TT in a Portuguese cohort of AHCM patients. Our main finding is the potential role of longitudinal strain rate in apical segments as an independent predictor of adverse events in this population.

In our cohort, only 56,9% of patients had a suspected diagnosis of AHCM based on echocardiography, corroborating its lower diagnostic accuracy compared to CMR [7]. Still, it should be noted that only seven patients underwent TTE with ultrasonographic contrast. CMR proved to be a reliable imaging method to characterize the location, distribution and extent of LVH [3, 7, 13]. LV mass index was normal, despite a maximum LV wall thickness of 15 mm. However, when hypertrophy is limited and segmental, LV mass calculated by CMR is usually within normal limits, underscoring that cardiac mass is not a diagnostic prerequisite for HCM [3]. In our population, only one patient (2%) had an apical aneurysm, reflecting a minor proportion comparing to other studies, where its prevalence reaches 15% [4, 15].

LGE was present in 78,4%, mainly restricted to the hypertrophied apical segments. This prevalence overcomes the data reported in other AHCM studies, where it ranges between 40 and 70% [2–5, 7], even with a large proportion of the “relative form” in our population. In the largest available series of AHCM patients imaged with CMR [18], LGE was also limited to the hypertrophic apical segments. Several large studies show a significant linear relationship between the extent of LGE (particularly if $\geq 15\%$ of LV mass) and the risk of SCD in HCM [3].

While not negligible, our data demonstrated a low incidence of adverse cardiac events and a low mortality in AHCM patients, in concordance with previous studies [15]. Patients that suffered an adverse event were older, had a

Fig. 2 Cardiac magnetic resonance imaging showing left ventricle hypertrophy at the apex (measuring 15 mm), compatible with apical hypertrophic cardiomyopathy

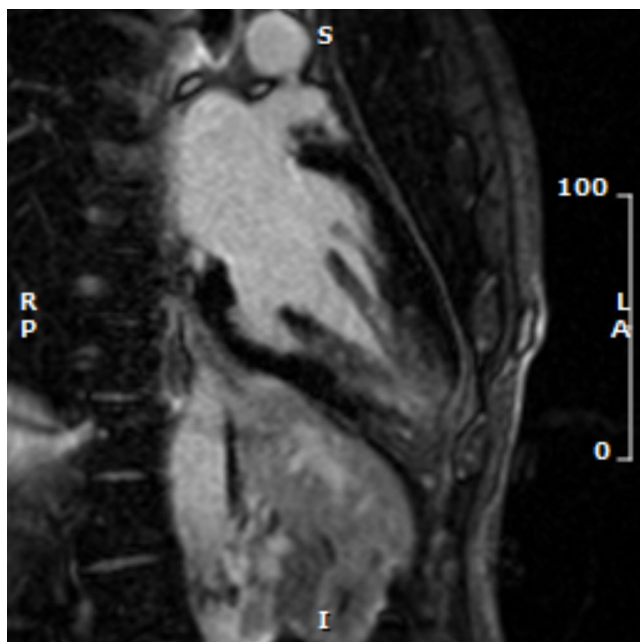
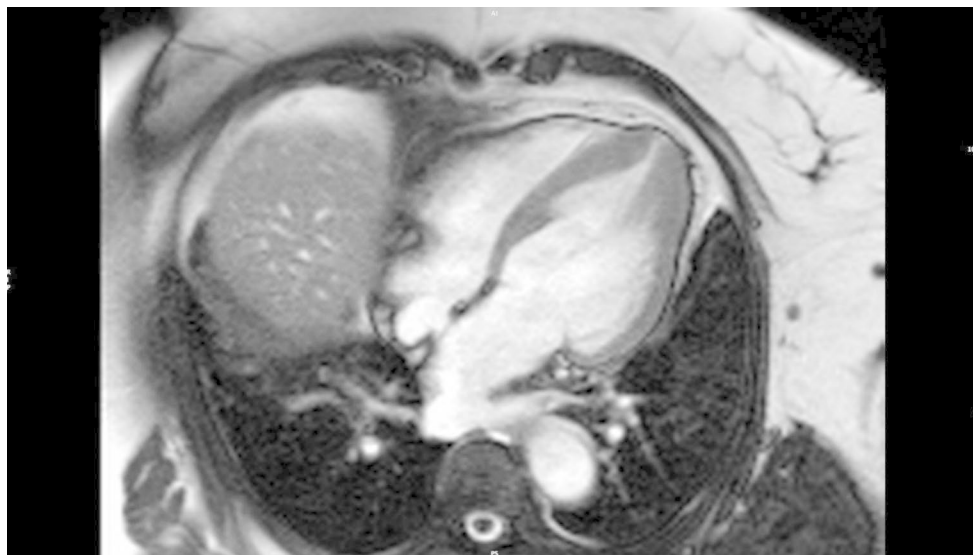


Fig. 3 Cardiac magnetic resonance imaging of patient with apical hypertrophic cardiomyopathy, showing late gadolinium enhancement at the left ventricle apex

larger prevalence of COPD, and lower longitudinal strain rate in apical segments. Although LGE and GLS have been associated to an increased risk of VA and SCD [1, 19], neither parameter was associated with the primary endpoint. After multivariable analysis, only longitudinal strain rate in apical segments was an independent predictor of the primary endpoint.

In the study of Pu et al. [1], involving HCM patients, reduced GLS derived by CMR-TT was an independent predictor for VA, as well as the percentage of LGE. A recent HCM meta-analysis also demonstrated an association

Table 3 CMR-TT analysis of AHCM patients

CMR parameters	Total n=46
Global longitudinal strain (%), median	-14,37
Global radial strain (%), median	30,35
Global circumferential strain (%), median	-18
Global longitudinal strain rate (%), median	-0,73
Global radial strain rate (%), median	1,39
Global circumferential strain rate (%), median	-0,90
Time to peak (longitudinal strain) (ms), median	336,6
Torsion (°/cm), median	0,7
Torsion rate (°/s), median	5,15

AHCM=Apical hypertrophic cardiomyopathy; CMR-TT=Cardiac magnetic resonance tissue-tracking

between GLS and a composite endpoint of adverse cardiovascular events [3]. However, its strength as a clinical predictor remains limited by substantial variability in methodology, as well as the absence of adequately powered prospective clinical studies. In addition, Li et al. [16] reported global longitudinal peak diastolic strain rate as an early index of LV diastolic function providing prognostic information in HCM patients.

This is the first Portuguese study addressing myocardial deformation parameters derived by CMR-TT in AHCM patients. We highlight the potential role of CMR-TT strain parameters as significant prognostic factors, since longitudinal strain rate in apical segments predicted all-cause hospitalizations and mortality in our cohort. While aiming to improve the risk stratification in AHCM patients, we also reinforce the important role of CMR in diagnosing AHCM and explore the long-term prognosis of these patients. Future larger multicentre studies with prospective selection of AHCM patients are needed to establish standardized parameters for CMR-TT and to better explore their

Table 4 Comparison between patients with and without the primary endpoint (PE)

Characteristics	Patients with PE (n=10)	Patients without PE (n=37)	p-value
Age (years-old), mean ± SD	69,2 ± 8,2	59,5 ± 14,4	0,01
Male gender (%)	40	64,9	0,155
Arterial hypertension (%)	80	59,5	0,230
Diabetes mellitus (%)	40	29,7	0,536
Atrial fibrillation (%)	20	16,2	0,778
Coronary artery disease (%)	10	13,5	0,768
Chronic kidney disease (%)	0	5,4	0,452
Chronic obstructive pulmonary disease (%)	20	2,7	0,047
Syncope (%)	10	2,9	0,346
Maximal LV thickness (mm), mean ± SD	15,6 ± 2,9	14,5 ± 4,0	0,357
LV mass index (g/m ²), mean ± SD	76,9 ± 20,0	76,4 ± 18,4	0,948
Apical aneurysm (%)	0	2,7	0,599
Late gadolinium enhancement (%)	80	78,4	0,911
Global longitudinal strain (%), mean ± SD	-13,3 ± 3,9	-14,2 ± 3,4	0,548
• Basal LS (%), mean ± SD	-21,2 ± 3,6	-21,5 ± 3,7	0,858
• Medium LS (%), mean ± SD	-12,8 ± 5,6	-13,7 ± 3,4	0,617
• Apical LS (%), mean ± SD	-5,5 ± 4,6	-8,2 ± 5,1	0,137
Global radial strain (%), mean ± SD	31,8 ± 7,6	28,7 ± 6,4	0,267
• Basal RS (%), mean ± SD	33,2 ± 11,4	34,7 ± 8,1	0,692
• Medium RS (%), mean ± SD	32,7 ± 10,3	28,7 ± 6,5	0,266
• Apical RS (%), mean ± SD	19,1 ± 14,9	18,6 ± 13,2	0,920
Global circumferential strain (%), mean ± SD	-18,3 ± 3,3	-17,2 ± 2,7	0,366
• Basal CS (%), mean ± SD	-19,9 ± 3,1	-19,3 ± 2,0	0,593
• Medium CS (%), mean ± SD	-19,4 ± 3,7	-17,8 ± 2,7	0,214
• Apical CS (%), mean ± SD	-11,1 ± 5,5	-12,2 ± 6,5	0,584
Global longitudinal strain rate (%), mean ± SD	-0,40 ± 0,74	-0,98 ± 1,19	0,08
• Basal LSR (%), mean ± SD	-0,64 ± 1,17	-1,24 ± 0,42	0,143
• Medium LSR (%), mean ± SD	-0,81 ± 0,19	-1,10 ± 1,39	0,265
• Apical LSR (%), mean ± SD	0,27 ± 1,06	-0,74 ± 1,24	0,021
Global radial strain rate (%), mean ± SD	1,65 ± 0,89	1,47 ± 0,53	0,534
• Basal RSR (%), mean ± SD	2,10 ± 0,68	1,75 ± 0,74	0,186
• Medium RSR (%), mean ± SD	2,04 ± 1,52	1,66 ± 0,80	0,463
• Apical RSR (%), mean ± SD	1,11 ± 0,84	1,31 ± 1,00	0,526
Global circumferential strain rate (%), mean ± SD	-0,98 ± 0,82	-1,02 ± 0,43	0,884
• Basal CSR (%), mean ± SD	-0,69 ± 1,07	-1,08 ± 0,46	0,288
• Medium CSR (%), mean ± SD	-1,17 ± 0,86	-1,17 ± 0,73	0,984
• Apical CSR (%), mean ± SD	-1,00 ± 0,89	-1,04 ± 0,67	0,923
Time to peak (longitudinal strain) (ms), mean ± SD	356,6 ± 89,0	339,3 ± 49,6	0,569
Torsion (°/cm), mean ± SD	0,79 ± 0,64	0,782 ± 0,36	0,970
Torsion rate (°/s), mean ± SD	6,44 ± 3,37	6,19 ± 2,99	0,839

LV=Left ventricle; CS=Circumferential strain; CSR=Circumferential strain rate; LS=Longitudinal strain; LSR=Longitudinal strain rate; RS=Radial strain; RSR=Radial strain rate; SD=Standard deviation

prognostic significance, in order to improve risk stratification in this population.

Limitations

Some limitations were encountered during our study. First, it has a retrospective design, susceptible to inherent bias. Also, the relatively small number of patients from a single medical centre limits the interpretation of the results. Moreover, some patients were lost to follow-up, resulting in loss of information regarding adverse events. Finally, our analysis was performed using a CMR-TT program from a single vendor, limiting the extrapolation of the results to other softwares.

Author contributions R.M.F and M.B wrote the main manuscript text. R.L.L, R.F and N.D.F did the CMR analysis of all the patients included in the study, and R.M.F performed the tissue-tracking analysis. All authors reviewed the manuscript and R.F.C revised the final version of the manuscript. All authors read and approved the final manuscript.

Funding None.

Declarations

Competing interests The authors declare no competing interests.

Conflict of interest None declared.

References

- Pu C, Fei J, Lv S et al (2021) Global circumferential strain by Cardiac magnetic resonance tissue tracking Associated with ventricular arrhythmias in hypertrophic cardiomyopathy patients. *Front Cardiovasc Med* 8(May):1–8. <https://doi.org/10.3389/fcvm.2021.670361>
- Parisi R, Mirabella F, Secco GG, Fattori R (2014) Multimodality imaging in apical hypertrophic cardiomyopathy. *World J Cardiol* 6(9):916. <https://doi.org/10.4330/wjc.v6.i9.916>
- Rowin EJ, Maron BJ, Maron MS (2020) The hypertrophic cardiomyopathy phenotype viewed through the prism of Multimodality Imaging: clinical and etiologic implications. *JACC Cardiovasc Imaging* 13(9):2002–2016. <https://doi.org/10.1016/j.jcmg.2019.09.020>
- Hughes RK, Knott KD, Malcolmson J et al (2020) Apical hypertrophic cardiomyopathy: the variant less known. *J Am Heart Assoc* 9(5):1–11. <https://doi.org/10.1161/JAHA.119.015294>
- Fattori R, Biagini E, Lorenzini M, Buttazzi K, Lovato L, Rapezzi C (2010) Significance of magnetic resonance imaging in apical hypertrophic cardiomyopathy. *Am J Cardiol* 105(11):1592–1596. <https://doi.org/10.1016/j.amjcard.2010.01.020>
- Yang H, Carasso S, Woo A et al (2010) Hypertrophy pattern and regional myocardial mechanics are related in septal and apical hypertrophic cardiomyopathy. *J Am Soc Echocardiogr* 23(10):1081–1089. <https://doi.org/10.1016/j.echo.2010.06.006>
- Huang G, Fadl SA, Sukhotski S, Matesan M (2019) Apical variant hypertrophic cardiomyopathy “multimodality imaging evaluation. *Int J Cardiovasc Imaging* 36(3):553–561. <https://doi.org/10.1007/s10554-019-01739-x>
- Moon JCC, Fisher NG, McKenna WJ, Pennell DJ (2004) Detection of apical hypertrophic cardiomyopathy by cardiovascular magnetic resonance in patients with non-diagnostic echocardiography. *Heart* 90(6):645–649. <https://doi.org/10.1136/hrt.2003.014969>
- Kao YC, Lee MF, Mao CT et al (2013) Differences of left ventricular systolic deformation in hypertensive patients with and without apical hypertrophic cardiomyopathy. *Cardiovasc Ultrasound* 11(1):1–12. <https://doi.org/10.1186/1476-7120-11-40>
- Hughes RK, Knott KD, Malcolmson J et al (2020) Advanced Imaging Insights in apical hypertrophic cardiomyopathy. *JACC Cardiovasc Imaging* 13(2P2):624–630. <https://doi.org/10.1016/j.jcmg.2019.09.010>
- Lee D, Montazeri M, Bataiosu R et al Clinical characteristics and prognostic importance of left ventricular apical aneurysms in hypertrophic cardiomyopathy. *JACC Cardiovasc Imaging*. 15(10):1696–1711
- Rickers C, Wilke NM, Jerosch-Herold M et al (2005) Utility of cardiac magnetic resonance imaging in the diagnosis of hypertrophic cardiomyopathy. *Circulation* 112(6):855–861. <https://doi.org/10.1161/CIRCULATIONAHA.104.507723>
- Gaudio C, Pelliccia F, Tanzilli G, Mazzarotto P, Cianfrocca C, Marino B (1992) Magnetic resonance imaging for assessment of apical hypertrophy in hypertrophic cardiomyopathy. *Clin Cardiol* 15(3):164–168. <https://doi.org/10.1002/clc.4960150306>
- Ünlü S, Özden Tok Ö, Avcı Demir F, Papadopoulos K, Monaghan MJ (2021) Differential diagnosis of apical hypertrophic cardiomyopathy and apical displacement of the papillary muscles: a multimodality imaging point of view. *Echocardiography* 38(1):103–113. <https://doi.org/10.1111/echo.14895>
- Kim EK, Lee SC, Hwang JW et al (2016) Differences in apical and non-apical types of hypertrophic cardiomyopathy: a prospective analysis of clinical, echocardiographic, and cardiac magnetic resonance findings and outcome from 350 patients. *Eur Heart J Cardiovasc Imaging* 17(6):678–686. <https://doi.org/10.1093/ehjci/jev192>
- Li ZL, He S, Xia CC et al (2021) Global longitudinal diastolic strain rate as a novel marker for predicting adverse outcomes in hypertrophic cardiomyopathy by cardiac magnetic resonance tissue tracking. *Clin Radiol* 76(1):78. e19–78.e25
- CVI42 - User manual Version 5.5. Connect (2016) :1-241. https://www.circlecvi.com/docs/product-support/manuals/cvi42_user_manual_v5.5.pdf
- Masao Yamada K, Teraoka M, Kawade, Masaharu Hirano AY (2009) Frequency and distribution of late gadolinium enhancement in magnetic resonance imaging of patients with apical hypertrophic cardiomyopathy and patients with asymmetrical hypertrophic cardiomyopathy: a comparative study. *Int J Cardiovasc Imagin* 25(Suppl 1):131–138
- Pelletier R, Choi J, Winters N et al (2016) Sex differences in clinical outcomes after premature Acute Coronary Syndrome. *Can J Cardiol* 32(12):1447–1453. <https://doi.org/10.1016/j.cjca.2016.05.018>

Publisher's Note Springer Nature remains neutral with regard to jurisdictional claims in published maps and institutional affiliations.

Springer Nature or its licensor (e.g. a society or other partner) holds exclusive rights to this article under a publishing agreement with the author(s) or other rightsholder(s); author self-archiving of the accepted manuscript version of this article is solely governed by the terms of such publishing agreement and applicable law.